



Published in final edited form as:

Chem Res Toxicol. 2016 December 19; 29(12): 2125–2135. doi:10.1021/acs.chemrestox.6b00233.

4-Hydroxy-7-oxo-5-heptenoic Acid (HOHA) Lactone Induces Angiogenesis through Several Different Molecular Pathways

Junhong Guo¹, Mikhail Linetsky¹, Annabelle O. Yu², Liang Zhang³, Scott J. Howell⁴, Heather J. Folkwein¹, Hua Wang¹, and Robert G. Salomon^{1,*}

¹Department of Chemistry, Case Western Reserve University, Cleveland, Ohio, 44106, USA

²Department of Biology, Case Western Reserve University, Cleveland, Ohio, 44106, USA

³Department of Biochemistry, Case Western Reserve University, Cleveland, Ohio, 44106, USA

⁴Department of Ophthalmology and Visual Sciences, Case Western Reserve University, Cleveland, Ohio, 44106, USA

Abstract

Oxidative stress and angiogenesis have been implicated not only in normal phenomena such as tissue healing and remodeling but also in many pathological processes. However, the relationships between oxidative stress and angiogenesis still remain unclear, although oxidative stress has been convincingly demonstrated to influence the progression of angiogenesis under physiological and pathological conditions. The retina is particularly susceptible to oxidative stress owing to its intensive oxygenation and high abundance of polyunsaturated fatty acyls. In particular, it has high levels of docosahexaenoates whose oxidative fragmentation produces 4-hydroxy-7-oxo-5-heptenoic acid (HOHA)-lactone. Previously, we found that HOHA-lactone is a major precursor of 2-(ω -carboxyethyl)pyrrole (CEP) derivatives that are tightly linked to age-related macular degeneration (AMD). CEPs promote the pathological angiogenesis of late stage AMD. We now report additional mechanisms by which HOHA-lactone promotes angiogenesis. Using cultured ARPE-19 cells; we observed that HOHA-lactone induces secretion of vascular endothelial growth factor (VEGF), which correlated to increases in reactive oxygen species (ROS) and decreases in intracellular glutathione (GSH). Wound healing and tube formation assays provided, for the first time, in vitro evidence that HOHA-lactone induces the release from ARPE-19 cells of VEGF that promotes angiogenesis by human umbilical vein endothelial cells (HUVEC) in culture. Thus, HOHA-lactone can stimulate vascular growth through a VEGF-dependent pathway. In addition, results from MTT and wound healing assays as well as tube formation experiments showed that GSH-conjugated metabolites of HOHA-lactone stimulate HUVE cell proliferation and promote angiogenesis in vitro. Previous studies demonstrated that HOHA-lactone, through its CEP derivatives, promotes angiogenesis in a novel Toll-like receptor 2-dependent manner that is

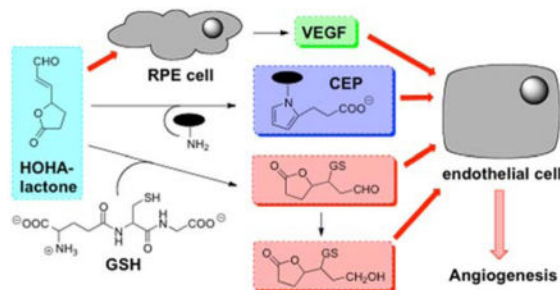
*To whom correspondence should be addressed at Department of Chemistry, Case Western Reserve University, Cleveland, Ohio 44106-7078; rgs@case.edu, Phone: 216-368-2592. FAX: 216-368-3006.

SUPPORTING INFORMATION

Figure S1. The pro-angiogenic effect of HOHA-lactone-GSH (-OH) on HUVEC in the wound healing assay; Figure S2. The pro-angiogenic effect of HOHA-lactone-GSH (=O) on HUVEC in the tube formation assay; Figure S3. Effect of RPE conditioned medium on HUVECs in a tube formation assay in the absence and in the presence of Avastin (20 μ g/ml) or AAL-993 (100 nM). This material is available free of charge via the Internet at <http://pubs.acs.org>.

independent of the VEGF receptor or VEGF expression. The new studies show that HOHA-lactone also participates in other angiogenic signaling pathways that include promoting the secretion of VEGF from RPE cells.

Graphical abstract



Keywords

Angiogenesis; oxidative stress; age-related macular degeneration; vascular endothelial growth factor; retinal pigment epithelium cells; HOHA-lactone

INTRODUCTION

The retina, a light-sensitive layer that lines the back of the eye, is particularly susceptible to oxidative damage owing to its intensive oxygenation and high levels of polyunsaturated fatty acids (PUFAs).¹⁻³ The retinal pigmented epithelium (RPE) plays critical roles not only in the maintenance of the normal functions of the retina and also in the homeostasis of different retinal structures like photoreceptors or choriocapillaries by secreting various growth factors including vascular endothelial growth factor (VEGF).^{2, 4} Dysfunction of the RPE has been implicated in the pathogenesis of many retinal diseases, including retinitis pigmentosa and age-related macular degeneration (AMD).^{1, 2, 5}

Angiogenesis is the formation of new blood vessels from pre-existing blood vessels, which plays a central role in physiological processes such as embryogenesis and wound healing and is important for the progression of cancer, and chronic inflammation.⁶ VEGF promotes angiogenesis in tumors and also in the retinal microenvironment.^{5, 7} In the retina, VEGF is essential for the development of retinal and choroidal vascularization as well as the neuroretina.⁵ However, VEGF is now emerging as a risk factor for AMD wherein vascular hyperpermeability and neovascularization are observed.⁸ VEGF levels are significantly increased in retinas and plasma of AMD subjects.^{8, 9} RPE cells have been suggested to be the source of VEGF that promotes the choroidal neovascularization observed in AMD.⁵ The successful clinical application of the anti-VEGF compounds bevacizumab, ranibizumab, and pegaptanib in AMD strongly supports the importance of VEGF in progression of neovascular AMD.^{2, 10, 11} However, the stimuli leading to enhanced VEGF release from RPE cells and the subsequent neovascularization in AMD remain unclear.

Oxidative stress is considered to be the major detrimental factor that causes AMD.^{11, 12} Under oxidative stresses, PUFAs, especially docosahexaenoic acid (DHA), an omega-3 fatty acid that comprises 60% of the PUFAs in the retina, undergo oxidation and truncation to generate a multitude of reactive aldehydes, which include 3-(5-oxotetrahydrofuran-2-yl)acrylaldehyde (HOHA-lactone) (Scheme 1).^{3, 13} Recently, this α,β -unsaturated aldehyde was shown to react with the primary amino groups of biomolecules to produce carboxyethylpyrrole (CEP) derivatives of proteins and ethanolamine phospholipids.¹⁴ CEP was found to be more abundant in AMD than in normal Bruch's membrane/RPE/choroid tissues.¹⁵ The levels of CEP derivatives were shown to be elevated in human plasma from AMD donors relative to normal healthy donors.^{16, 17} Animal model studies also demonstrated that CEP derivatives stimulate choroidal neovascularization and promote wound healing and tumor growth through toll-like receptor 2 (TLR2) signaling.^{18, 19} In addition, we recently observed that RPE cells take up HOHA-lactone, conjugate it with glutathione (GSH) to form HOHA-lactone-GSH (=O). The aldehyde is then reduced to HOHA-lactone-GSH (-OH) that is secreted (Scheme 1).²⁰

Oxidative stress has been found not only to increase the production of VEGF but also to be involved in the upregulation of VEGF expression.^{6, 21–23} Reactive oxygen species (ROS)^{21, 22, 24} and lipid peroxidation products including oxidized phospholipids (OxPLs)²⁵, malondialdehyde (MDA)²³ and 4-hydroxy-2-nonenal (4-HNE)^{26–28}, induce secretion of VEGF by RPE cells. Interestingly, ROS and 4-HNE seem to have biphasic effects in regard to cellular activity; low levels of ROS and 4-HNE induce proliferation and growth of vascular endothelial cells, but high levels of ROS and 4-HNE stimulate apoptosis.^{27–29} Similar to the reported hormetic effect of 4-HNE,²⁸ our recent studies showed that HOHA-lactone, a structural analog that incorporates the electrophilic functionality of 4-HNE, promotes VEGF secretion at low concentrations, and inhibits this secretion at high concentrations in a human retinal pigmented epithelial cell line (ARPE-19), a spontaneously formed cell line from human RPE cells that is widely used to investigate the expression of VEGF.¹⁴ These findings pose an intriguing question as to how HOHA-lactone is able to exert such a multitude of effects on cellular processes.

Since elevated oxidative stress and VEGF levels as well as reduced plasma GSH were observed with AMD,^{26, 29} one objective of the present study was to determine whether HOHA-lactone depletes GSH and thus induces oxidative stress and VEGF secretion in ARPE-19 cells. To this end, we systematically investigated the dose-dependent effect of HOHA-lactone on cell viability, VEGF secretion, intracellular GSH levels, and oxidative stress. A second objective was to determine the biological consequences of HOHA-lactone-induced VEGF secretion from RPE cells. To this end, the effects of HOHA-lactone induced VEGF secreted from RPE cells on migration and tube formation of human umbilical vein endothelial cells (HUVEC) in matrigel were examined in vitro. Moreover, the cytotoxicity of GSH conjugates of HOHA-lactone (HOHA-lactone-GSH (=O) and GSH-HOHA-lactone (-OH)) as well as their biological activities were also examined in vitro. To this aim, the pro-angiogenic properties of GSH conjugates of HOHA-lactone toward HUVEC were studied. The results of these studies show, for the first time, that HOHA-lactone promotes angiogenesis by HUVEC through several pathways. Combined with the previous results that HOHA-lactone serves as an important precursor of CEP derivatives, which also promote

angiogenesis, we conclude that HOHA-lactone may contribute to choroidal neovascularization either through direct interaction with RPE cells to induce secretion of VEGF that then promotes angiogenesis in surrounding vascular endothelial cells or through adduction with GSH to form GSH conjugates or through the formation of CEPs that promote angiogenesis in a TLR2-dependent manner.

Materials and Methods

Reagents

Dulbecco's modified Eagle's medium (DMEM)/F12, Dulbecco's phosphate buffered saline (DPBS), Hank's balanced salt solution (HBSS), fetal bovine serum (FBS) and 2',7'-dichlorodihydrofluorescein diacetate (DCFHDA) were purchased from Fisher Scientific (Pittsburgh, PA). A human VEGF-A ELISA kit was purchased from Pierce and Warriner (Pittsburgh, PA). A human VEGF-A ELISA kit was purchased from Pierce and Warriner (Pittsburgh, PA). A human VEGF-A ELISA kit was purchased from Pierce and Warriner (Pittsburgh, PA). Retinal pigmented epithelial cell basal medium (RtEBM), an optimized mixture of growth factors and supplements for primary hRPE cells (SingleQuots™ Kit) was obtained from Lonza (Allendale, NJ). Goat anti rabbit FITC antibody and 3-(4,5-dimethylthiazol-2-yl)-2,5-diphenyltetrazolium bromide (MTT) were obtained from Invitrogen (Carlsbad, CA). All other chemicals and reagents including L-glutathione (reduced), sodium borohydride, glutathione reductase (250 units ml⁻¹), 5,5'-dithio-bis(2-nitrobenzoic acid) (DTNB), and β-NADPH, etc. were purchased from Sigma-Aldrich (St. Louis, MO). The lactone of 4-hydroxy-7-oxohept-5-enoic acid (HOHA-lactone) was synthesized as described previously.³⁰ The purity of HOHA-lactone was 98.6% (¹H NMR).

Cell Lines

The human retinal pigmented epithelial cell line (ARPE-19), obtained from the American Type Culture Collection (ATCC, CRL-2302), was sub-cultured in DMEM/F12 containing 10% FBS and antibiotics in a humidified incubator at 37 °C in 5% CO₂ atmosphere. Human umbilical vein endothelial cells (HUVEC) were obtained from PromoCell (Heidelberg, Germany). The cell line and the primary cells were trypsinized and passaged every 2–3 days (passages 20–27 have been used for ARPE-19 cells and passages 3–5 were used for HUVEC throughout this project). Clonetics™ human primary retinal pigmented epithelial cells (hRPE) (passage 2) were obtained from Lonza (Allendale, NJ) and maintained and sub-cultured in RtEBM supplemented with the optimized mixture of growth factors and supplements and 10% heat-inactivated FBS. hRPE cells were passaged every 4–5 days and passages 3–5 were used throughout this project.

Microscopy

Images were collected on a Leica DMI 6000B inverted fluorescence microscope (Leica Microsystems Wetzlar, Germany) using a Retiga EXI camera (Q-imaging, Vancouver, British Columbia). Image analysis was performed using MetaMorph Imaging Software (Molecular Devices, Downingtown, PA). The images are representative of four independent experiments that showed very similar results.

Cell Viability

The ARPE-19 or HUVEC (4.5×10^4 cells per well) were seeded in 96-well plates in DMEM/F12 or HUVEC cell culture medium supplemented with 10% heat-inactivated FBS, respectively, and incubated at 37 °C, under 5% CO₂ overnight. After starving the cells for 4 to 5 hours in a basal medium, 200 µl of basal cell culture medium containing various concentrations of HOHA-lactone or HOHA-lactone-GSH conjugates (0–100 µM) were added. After incubation at 37 °C, under 5% CO₂ overnight (about 16 h), the cell viability was estimated by running an MTT assay for both HOHA-lactone and HOHA-lactone-GSH conjugates and lactate dehydrogenase (LDH, Thermo Scientific) assay only for HOHA-lactone according to the manufacturer's instructions.

For the MTT assay, at the end of the overnight incubation, the supernatants were removed and the cells were washed with basal cell culture medium three times and then incubated with in 180 µL of basal medium supplemented with 20 µL of sterile MTT solution (5 mg/ml in basal medium) at 37 °C under 5% CO₂ for 4 h. The plates were then centrifuged at 1,000g for 5 min using a swinging bucket rotor equipped with microplate carriers and the medium was aspirated from microplate wells. Dimethylsulfoxide (DMSO; 200 µL) of was added to each well, thoroughly mixed and the absorbance in wells was measured by using a plate reader (Model M3, Molecular Devices) at the wavelength set at $\lambda = 570$ nm and a reference wavelength set at $\lambda = 670$ nm.

The LDH assay was conducted according to the manufacturer's instructions. Briefly, after overnight incubation, the 96-well microplates, containing ARPE-19 cells (non-challenged and challenged with HOHA-lactone) were then centrifuged at 1,000g for 5 min using a swinging bucket rotor equipped with microplate carriers and the supernatants were collected. 100 µL of each sample was transferred to a 96-well plate and mixed with 100 µL of LDH reagent mixture. After incubation for another 30 min at room temperature, 50 µL of stop solution was added and the absorbance of samples was measured at the wavelengths set at $\lambda_1=490$ nm and a reference wavelength set at $\lambda = 670$ nm (to subtract any absorbance caused by light scattering in samples).

Measurement of Oxidative Stress

Intracellular oxidative stress in ARPE-19 cells was measured using the DCFHDA probe as described elsewhere.³¹ Briefly, 4.5×10^4 ARPE-19 cells were seeded in 8-chamber slides (LabTek II) in the complete DMEM/F12 culture medium overnight at 37 °C under 5% CO₂. ARPE-19 cells were starved on the following day in a basal DMEM/F12 medium for 4 to 5 hours. Then cells were pre-incubated with 13.3 µM DCFHDA for 45 min, washed with warm basal medium and further incubated with 0–30 µM HOHA-lactone for another 30 min at 37 °C, under 5% CO₂. The images were collected on a Leica DMI 6000B inverted fluorescence microscope as described above.

Estimation of VEGF Secretion from ARPE-19 cells

Starved ARPE-19 cells grown in 96-well plates (2.5×10^4 cells per well) were incubated with 200 µL of basal DMEM/F12 media containing various concentrations (0–25 µM) of HOHA-lactone. After 16 h of incubation, supernatants were collected to estimate secreted VEGF-A

using an enzyme-linked immunosorbent assay (ELISA) according to the manufacturer's protocol (human VEGF-A ELISA kit, Pierce, Rockford, IL). Absorbance was measured using a plate reader (Molecular Devices) with the wavelength set at $\lambda = 450$ nm and a reference wavelength set at $\lambda = 670$ nm.

Estimation of Intracellular GSH in ARPE-19 cells

Determination of intracellular GSH was conducted using Ellman's reagent, 5,5'-dithio-bis(2-nitrobenzoic acid) (DTNB) as described elsewhere.³² Briefly, 2×10^6 of ARPE-19 cells were grown in 60 mm tissue culture dishes and washed with basal DMEM/F12 medium. Basal medium (3 mL) containing different concentrations of HOHA-lactone (0–25 μ M) was added to the cell culture dishes and incubated for 2 h at 37 °C, under 5% CO₂. At the end of the incubation, the cell tissue culture dishes were washed three times with the basal DMEM/F12 medium and aspirated. This was followed by the addition of 400 μ L of HBSS and the cells were scraped using a rubber policeman and collected in 5-ml conical tubes and centrifuged at 1,000g for 5 min using a swinging bucket rotor and placed on ice. After supernatants were aspirated, the cells were sonicated at 4 °C in cell lysis buffer (200 μ L) and designated as the "cell lysate". Aliquots (10 μ L) of ARPE cell lysates from dose-dependent studies were taken to estimate intracellular GSH using a colorimetric microplate method described previously.³³ Briefly, 10 μ L of blanks, GSH standards or samples were added to the corresponding wells, followed by the addition of 120 μ L of a freshly prepared mixture of DTNB (10 mM) and glutathione reductase (40 μ L (250 units/ml) Then, 60 μ L of β -NADPH (0.67 mg/ml) was added and mixed well. The plate was immediately placed in a microplate reader (Molecular Devices) and absorbance was measured at a wavelength of 412 nm after mixing for 2 min.

Wound Healing Assay

An in vitro wound-healing assay was performed using a previously described method with slight modifications.³⁴ In brief, HUVEC (initial seeding of 1×10^5 cells/well) were grown to 90–95% confluence in a 24-well cell tissue culture plate at 37 °C under 5% CO₂ overnight. The cell monolayer was scraped in a straight line to create a "scratch" with a sterile 200 μ L micropipette tip. Then the plate was carefully washed once with warm phenol red-free basal HUVEC cell culture medium and 450 μ L of basal HUVEC medium was added, followed by the addition to the corresponding wells of 50 μ L of HOHA-lactone-GSH conjugates or the conditioned media obtained from ARPE-19 cell cultures with or without HOHA-lactone treatment to make final concentrations from 0.1 μ M to 2.0 μ M. Cells were photographed (phase-contrast) at the start of the incubation (0 time) and 24 h after creating the scratch line. The images were collected using a Leica DMI 6000B inverted microscope as described above.

The "wound" distance was measured using five separate distance measurements that spanned from one "wound" edge to the other. These same five measurements were repeated at the 24 hour time point. To ensure that the same area was measured we included orientation marks on the plates themselves. By using these orientation marks we were able to image the same area of the "wound" at each time point and then perform the subsequent measurements by MetaMorph Imaging Software (Molecular Devices, Downingtown, PA).

Tube Formation Assay

An in vitro tube formation assay was conducted as described previously.³⁵ Briefly, HUVEC were incubated and starved overnight at 37 °C under 5% CO₂, scraped with a rubber policeman, counted and then seeded onto 48-well plates (2.5×10⁴ cells/well), which had been pretreated with growth factor-reduced (GFR) matrigel (Trevigen Inc., Gaithersburg, MD). Usually 175 µl/well of GFR (initial concentration is approximately 15 mg/ml) was incubated for 1 h at 37 °C to allow the gel to solidify at room temperature for 2 h. Then HOHA-lactone-GSH conjugates or the conditioned media obtained from ARPE-19 cells which were incubated with or without HOHA-lactone treatment were added to the corresponding microplate wells to make final concentrations between 0.1 µM to 2.0 µM. HUVEC were incubated overnight at 37 °C under 5% CO₂. The following day, cells were stained with Calcein AM (BD Biosciences) solution by adding 50 µL of working solution (0.01 mg/ml) to each well. After incubating for 45 min at 37 °C and gently washing the wells with warm HUVEC basal medium, images were collected using a Leica DMI 6000B inverted fluorescence microscope (FITC filter, Leica Microsystems Wetzlar, Germany) equipped with a Retiga EXI camera (Q-imaging, Vancouver, British Columbia). All the measurements (tube lengths) were conducted using MetaMorph Imaging Software (Molecular Devices, Downingtown, PA).

Chemical Synthesis of HOHA-lactone-GSH Conjugates

HOHA-lactone-GSH (=O) was synthesized by reacting 100 µmol of HOHA-lactone with 200 µmol of reduced glutathione in 3.0 mL water at room temperature for 3 h. Excess of GSH was removed by solid-phase extraction (SPE) through a Strata-X 33U polymeric reversed phase cartridge (Phenomenex, 500 mg/6ml). The cartridge was prewetted with 6 mL of methanol containing 0.1% formic acid and equilibrated with 6 mL of water containing 0.1% formic acid. After loading the sample, the cartridge was rinsed with 12 mL of water containing 0.1% formic acid to remove excess GSH. The adduct was eluted with 18 mL of 10% acetonitrile containing 0.1% formic acid. Mass analysis of this compound by ESI-MS showed m/z calcd for C₁₇H₂₆N₃O₉S (M+H)⁺, 448.47, found 448.26. HOHA-lactone-GSH (-OH) was prepared by reduction of 10 µmol of HOHA-lactone-GSH (=O) with 12 µmol of sodium borohydride in 1.5 mL of PBS buffer (pH = 7.4) at 4 °C for 5 h. Then the excess NaBH₄ was destroyed by adding 2 µL of neat formic acid. HOHA-lactone-GSH (-OH) was purified by SPE as above for HOHA-lactone-GSH (=O). ESI-MS showed m/z calcd for C₁₇H₃₀N₃O₉S (M+H)⁺, 450.48, found 450.76. The purity of these compounds was at least 99% or higher based on RP-HPLC (λ=220 nm) and LC-ESI-MS analyses.

Statistical Analysis

Unless specified in the text or legends, comparisons were made using One-Way ANOVA followed by Bonferroni's corrected posttest multiple t-tests. Statistical significance is shown as "*" p<0.05, "***" p<0.001, "****" p<0.0001. Data are presented as mean ± SD.

Results

HOHA-lactone induces biphasic concentration dependent effects on the survival of ARPE-19 cells

An MTT assay was conducted to assess the toxicity HOHA-lactone. Exposure of ARPE-19 cells to HOHA-lactone elicited a biphasic response. Exposure to high concentrations of HOHA-lactone ($>10 \mu\text{M}$) significantly decreased cell viability, with $\text{LD}_{50} = 38.6 \mu\text{M}$. However, the toxicity of HOHA-lactone was not significant at lower concentrations ($< 10 \mu\text{M}$), with more than 90% cell viability after incubation overnight (Figure 1A). Presumably, low levels of HOHA-lactone ($0.1\text{--}10 \mu\text{M}$) increased the cell number while higher levels ($>10 \mu\text{M}$) decreased the cell number (Figure 1). More interestingly, submicromolar concentrations of HOHA-lactone apparently stimulated cell proliferation considerably. Cell viability above 100% was observed when ARPE-19 cells were incubated in the presence of $1\text{--}500 \text{ nM}$ HOHA-lactone. The maximum cell viability ($155 \pm 15\%$), which is significantly higher than control cells ($p\text{-value} < 0.0001$), was observed with 10 nM HOHA-lactone. These results show that low nanomolar concentrations of HOHA-lactone stimulate ARPE-19 cell proliferation, and only levels above $10 \mu\text{M}$ are toxic. We then examined whether the toxic effect of HOHA-lactone is the result of a damaging effect on the cell plasma membrane. The integrity of the plasma membrane was evaluated as indicated by the release of LDH from the cell cytosol to the extracellular cell culture medium. The effects of HOHA-lactone on LDH leakage from the ARPE-19 cells (Figure 1B) were consistent with the results of the MTT assay. Damage of the ARPE-19 cell plasma membrane was only detected at HOHA-lactone concentrations above $40 \mu\text{M}$ (Figure 1B).

HOHA-lactone induces VEGF secretion from ARPE-19 cells

Recent studies showed that 4-HNE exerts concentration dependent opposite effects on the secretion of VEGF from RPE cells. At low levels, 4-HNE causes increased secretion of VEGF from RPE cells, but at higher concentration it inhibits VEGF secretion.²⁸ Because HOHA-lactone is a structural analog of 4-HNE, we tested whether HOHA-lactone stimulates the secretion of VEGF by RPE cells. ARPE-19 cells were exposed to various concentrations of HOHA-lactone, and VEGF levels in the extracellular medium were measured. We found that HOHA-lactone induces VEGF secretion by ARPE-19 cells in a dose-dependent manner. HOHA-lactone at concentrations of 0.1 to $10 \mu\text{M}$ induced significant increases over the level of VEGF secreted by untreated (control) ARPE-19 cells ($1295 \pm 50 \text{ pg/ml}$). VEGF secretion by ARPE-19 cells reached a maximal level of $3168 \pm 125 \text{ pg/ml}$ (2.45-fold increase) upon exposure to $0.1 \mu\text{M}$ HOHA-lactone. However, exposure to high concentrations of HOHA-lactone, e.g., $25 \mu\text{M}$, significantly abrogated the secretion of VEGF (Figure 2).

Exposure of ARPE-19 cells to HOHA-lactone creates an environment that promotes migration and tube formation by HUVECs

Since VEGF is a primary inducer of cell migration that is necessary for neovascularization by endothelial cells,²⁸ the ability of ARPE-19 cells to promote angiogenesis after exposure to HOHA-lactone was tested using an in vitro migration (wound healing) assay with HUVEC.³⁴ Compared to conditioned medium (CM) from cells not treated with HOHA-

lactone, CM derived from HOHA-lactone treated ARPE-19 cells promoted a significantly higher level of migration (Figure 3). HUVEC maintained in the CM from ARPE-19 cells exposed to 0.1–2 μM HOHA-lactone for 24 h showed dose-dependent progressive reoccupation of the wounded region and reached the maximal level at 2 μM HOHA-lactone. These data provide, for the first time, clear in vitro evidence for HOHA-lactone-induced wound healing that is mediated through factors secreted by ARPE-19 cells.

To further investigate the pro-angiogenic effects of factors secreted from HOHA-treated ARPE-19 cells, the matrigel tube formation assay, which is a convenient and quantifiable method to test the vascular formation properties on HUVEC in vitro, was performed. As shown in Figure 4, treatment of HUVEC with CM from HOHA-lactone treated ARPE-19 cells increased the total length of tube-like structures in comparison with control CM. The photographs were image-analyzed and the total tube lengths were measured (Figure 4B). When the HUVEC were incubated with CM from ARPE-19 cells exposed to 0.1–1 μM HOHA-lactone, the tube length increased in a dose dependent manner and reached the greatest level at 0.25 μM HOHA-lactone. It should be noted, that pre-treatment of CM with Avastin (anti-VEGF antibody at 20 $\mu\text{g}/\text{ml}$ for 3 h at room temperature) before adding to HUVE cells in a standard tube formation assay decreased the tube formation by 47% and 26% in the CM from control cells and the CM from ARPE-19 treated with 1.0 μM HOHA-lactone, respectively. Furthermore, adding the VEGFR kinase inhibitor AAL-993 at a concentration (100 nM) sufficient to block VEGF-A signaling, to HUVE cells together with CM from ARPE-19 treated with 1.0 μM HOHA-lactone lowered tube formation by 39% (Fig. S3). These results further confirmed that the release of factors from HOHA-lactone treated ARPE-19 cells promote angiogenesis.

HOHA-lactone-induced VEGF secretion correlates with oxidative stress in ARPE-19 cells

HOHA-lactone is a structural analog of 4-HNE, which is known to induce VEGF secretion via formation of intracellular ROS.²⁶ To test the hypothesis that HOHA-lactone induces the secretion of VEGF through a similar mechanism, oxidative stress was measured in HOHA-lactone-treated ARPE-19 cells. As shown in Figure 5, HOHA-lactone exposure at 0.1–1.0 μM triggered a significant increase of ROS in ARPE-19 cells compared to the control untreated cells, as measured by the increase of oxidized 2',7'-dichlorodihydrofluorescein (DCF) fluorescence intensity formed as the result of DCFHDA oxidation. Compared to untreated ARPE-19 cells, the fluorescence intensity from DCF was found to have a 3.2-fold ($p < 0.0001$) and 8.5-fold increase by treatment ARPE-19 cells with 0.1 μM and 0.5 μM HOHA-lactone, respectively. These data established that exposure to HOHA-lactone causes high levels of oxidative stress in ARPE-19 cells that presumably plays a significant role in VEGF secretion induced by HOHA-lactone. Preloading of ARPE-19 cells by incubation with 10 mM N-acetyl-Cys for 3 h followed by an extensive wash, and incubation of these cells in the presence of HOHA-lactone, drastically reduced intracellular oxidative stress (Fig. 5, Panel B and Panel C) compared to untreated cells and concomitantly diminished secretion of VEGF into the extracellular medium to negligible levels (data not shown). These data are in good agreement with the observations that pretreatment of ARPE cells with N-acetyl cysteine abrogated the induction of intracellular oxidative stress upon treatment with oxidized carotenoids³⁶ and a similar antioxidant effect of cysteine on the

ability of ARPE-19 cells challenged with 4-HNE to secrete VEGF into the extracellular medium.³⁷

Exposure of ARPE-19 cells to HOHA-lactone depletes intracellular GSH

The induction of oxidative stress in ARPE-19 cells as the result of HOHA-lactone treatment was verified by determining levels of intracellular GSH before and after treatment. Previously, we found that HOHA-lactone readily enters ARPE-19 cells that rapidly metabolize it by conjugation with GSH.²⁰ As expected, we now find that treatment of ARPE-19 cells with HOHA-lactone for 2 h resulted in a concentration-dependent progressive decrease of the intracellular levels of GSH from 52.0 ± 2.5 nmol/mg protein at 0 μ M HOHA-lactone to 21.5 ± 0.5 nmol/mg protein at 10 μ M HOHA-lactone (Figure 6).

HOHA-lactone-GSH conjugates are not cytotoxic to HUVEC

As described above, high concentrations of HOHA-lactone are toxic and significantly decrease ARPE-19 cell viability. Our previous studies showed that RPE cells take up HOHA-lactone, conjugate it with glutathione (GSH) to form HOHA-lactone-GSH (=O).²⁰ The aldehyde is then reduced to HOHA-lactone-GSH (-OH) that is secreted (Scheme 1). Although it is well-known that conjugation with GSH is a major detoxification pathway, there is also evidence indicating that several classes of compounds are converted to cytotoxic, genotoxic, or mutagenic metabolites after conjugation with GSH.³⁸ Therefore, we examined whether GSH conjugated metabolites of HOHA-lactone are toxic. The cytotoxicity of HOHA-lactone-GSH (=O) and HOHA-lactone-GSH (-OH) toward HUVEC cells was evaluated based on its effects on cell viability. When the HUVEC were incubated overnight with various concentrations of HOHA-lactone-GSH conjugates, an increase in cell viability was observed for all concentration of HOHA-lactone-GSH conjugates tested, as compared to the untreated control (Figure 7). As shown in Figure 7, the dose-response curve for the effects of treating HUVEC with HOHA-lactone-GSH conjugates is biphasic. Although HOHA-lactone-GSH conjugates can stimulate proliferation of HUVEC, the ability of HOHA-lactone-GSH conjugates to induce proliferation was not significant at concentrations less than 1–10 μ M. However, treatment with higher concentrations of HOHA-lactone-GSH conjugates (>10 μ M for HOHA-lactone-GSH (=O) and 1 μ M for HOHA-lactone-GSH (-OH)) significantly increased cell viability, with the maximum of $137.5 \pm 7.0\%$ and $181.0 \pm 2.5\%$ cell viability for 75 μ M HOHA-lactone-GSH (=O) and 2.5 μ M HOHA-lactone-GSH (-OH), respectively. Taken together, these data suggested that HOHA-lactone-GSH conjugates are not toxic metabolites. Instead, at high concentrations (above 1–10 μ M) they apparently stimulate HUVEC cell proliferation.

HOHA-lactone-GSH conjugates induce HUVEC angiogenesis in vitro

Pro-angiogenic effects of HOHA-lactone-GSH conjugates on HUVEC were investigated with cell migration (wound healing) and tube formation assays. In a wound healing assay, HOHA-lactone-GSH (=O) accelerated wound closure in cultured HUVEC (Figure 8). HUVEC treated with HOHA-lactone-GSH (=O) at concentrations of 0.1 to 2 μ M in PBS showed significant dose-dependent increases of wound healing (Figure 8B) when compared with cells treated with PBS, with the maximal increase at 1 μ M HOHA-lactone-GSH (=O). HOHA-lactone-GSH (-OH), the primary HOHA-lactone metabolite produced by RPE cells,

also caused enhanced migration (wound healing) by cultured HUVEC (Figure S1) that reached a maximal effect at 0.25 μM (Figure S1B).

Exposure of HUVEC to HOHA-lactone-GSH (-OH) at concentrations between 0.1 and 2 μM (Figure 9) promoted tube-forming activity that increased significantly and reached the maximal level at 0.5 μM compared with control. Higher concentrations of HOHA-lactone-GSH (-OH) reduced the total tube length reaching that of the control (PBS-treated) cells at 2 μM . Treatment of HUVEC with HOHA-lactone-GSH (=O) at concentrations between 0.1 and 2 μM resulted in a maximal increase in the total tube length at 0.1 μM and a decrease to the level observed for control (PBS-treated) cells at 1 μM , and a further drop at 2 μM (Figure S2).

Discussion

Although AMD is the most common cause of legal blindness in the elderly population in developed countries, the cellular, biochemical, and molecular events contributing to the etiology of AMD remain poorly understood.^{16,18} Oxidative stress has long been suspected of contributing to the pathogenesis of AMD.^{11, 12} Direct evidence of oxidative damage in AMD includes elevated levels of ROS^{21, 22, 24} and retinal lipid peroxidation products such as 4-HNE,^{26–28} isolevuglandin^{39–41} and CEP adducts.^{15–17} The retina is particularly susceptible to oxidative damage owing to its intensive oxygenation and high levels of polyunsaturated fatty acids (PUFAs).^{1–3} Considering that DHA, the precursor of HOHA-lactone is present in abundance in the retina,^{3, 13} it is likely that HOHA-lactone may be an important mediator of retinal degeneration associated with aging. Because RPE damage is an early event in AMD, it is important to delineate the role of HOHA-lactone in the degeneration of RPE cells.

Angiogenesis can either promote host defense and tissue repair or exacerbate organ dysfunction resulting in pathological states.¹⁹ In the retina, VEGF, a major factor in angiogenesis, is constitutively secreted by RPE cells to exert its physiological functions. For example, VEGF is an important protective factor for retinal cells and the choroid and is essential for the development of retinal and choroidal vascularization.⁵ However, VEGF is emerging now as a pathogenic factor in several pathological retinal conditions, most notably in edema, retinopathy of prematurity and choroidal neovascularization.⁸ Overexpression of VEGF by RPE cells in the retina was suggested to be a factor responsible for the development of choroidal neovascularization in vivo. Recently, oxidative stress-causing agents and electrophiles like 4-HNE were found to significantly induce VEGF secretion from RPE cells.^{26, 28}

Given that 4-HNE, a structural analog of HOHA-lactone, stimulates angiogenesis by induction of VEGF secretion in vitro,^{26, 28} the present study was undertaken to investigate the potential roles of HOHA-lactone in fostering VEGF secretion by ARPE-19 cells, which in turn induces angiogenesis in HUVEC cells. The results of this study established that HOHA-lactone induces the secretion of VEGF from the human retina derived ARPE-19 cell line. Similar to the reported hormetic effect of 4-HNE on ARPE-19 cells, HOHA-lactone at low levels promotes VEGF secretion but inhibits this secretion at high levels. In addition, we

observed that HOHA-lactone induces oxidative stress in ARPE-19 cells, as indicated by increased fluorescence intensity from DCFDA, an oxidative stress probe. Moreover, following HOHA-lactone treatment, ARPE-19 cells showed decreased levels of GSH. These results establish that HOHA-lactone induces the production of ROS by ARPE-19 cells presumably owing to a depletion of intracellular glutathione in these cells. We also investigated the physiological consequences of the secretion of VEGF and the production of GSH-HOHA-lactone conjugates by ARPE-19 cells upon exposure to low levels of HOHA-lactone. Using wound healing and tube formation assays, we provided, for the first time, evidence for the release of VEGF by ARPE-19 cells treated in vitro with HOHA-lactone leading to increased angiogenesis in cultured HUVEC. These data establish that HOHA-lactone can stimulate vascular growth in HUVEC through a VEGF dependent pathway.

Because HOHA-lactone can be metabolized ARPE-19 cells to form HOHA-lactone-GSH conjugates that are secreted, the cytotoxicity of HOHA-lactone-GSH conjugates toward HUVEC was studied. Results from the MTT assay showed that exposure of HUVEC to low levels of HOHA-lactone-GSH conjugates did not significantly change the cell number while high levels apparently increased the cell number. Because HOHA-lactone-GSH conjugates can stimulate HUVEC cell proliferation, the possible proangiogenic effects of HOHA-lactone-GSH conjugates were also investigated by cell migration and tube formation assays. We demonstrated that exposure of HUVEC to HOHA-lactone-GSH conjugates increases both wound healing and tube formation activities in vitro. These results together with our previous observations indicated that, besides promoting the secretion of VEGF by RPE cells, HOHA-lactone promotes angiogenesis by its conversion by RPE cells into pro-angiogenic HOHA-lactone-GSH conjugates. Thus, while VEGF induces angiogenesis by HUVEC cells and we have established that HOHA-lactone promotes VEGF secretion by RPE cells, this is not the only pathway by which HOHA-lactone fosters angiogenesis. While Avastin blocked the VEGF pathway, it did not block the HOHA-lactone-GSH induced angiogenesis and possibly other as yet unidentified pathways as is evident from the data presented in Figure S3 that show that Avastin was only able to prevent approximately half of the effect of HOHA-lactone on tube formation by HUVECs.

These results, coupled with our previous discoveries that HOHA-lactone is a major precursor of CEP derivatives of proteins and ethanolamine phospholipids¹⁴ and that those CEP derivatives promote angiogenesis through a novel TLR2-dependent mechanism that is independent of VEGF expression,^{18, 19} strongly suggest that HOHA-lactone may induce angiogenesis by at least three different molecular mechanisms. One mechanism for stimulation of angiogenesis is that HOHA-lactone induces the secretion by epithelial cells of VEGF. Another two mechanisms are dependent either on the formation of HOHA-lactone-GSH conjugates or CEP derivatives, which are all pro-angiogenic. The proposed angiogenesis pathways mediated by HOHA-lactone are summarized in Figure 10.

The contribution of HOHA-lactone to angiogenesis may vary in different physiological settings, depending on the extent of oxidative stress. Low levels of HOHA-lactone may be generated as a consequence of low levels of oxidative stress and promote protective mechanisms in four different pro-angiogenic signaling pathways, thereby contributing to accelerated wound healing and tissue recovery in physiological settings. If high levels of

HOHA-lactone accumulate as a result of persistent oxidative stress in tissues, it may lead to excessive vascularization in the long run, for example, in tumors. Currently, anti-VEGF therapies are the standard of care for treating AMD and other vascular retinal diseases.^{2, 10, 11} Recently, anti-CEP therapy was suggested to be a promising treatment for cancers,¹⁹ especially in diseases resistant to anti-VEGF therapy. Here, HOHA-lactone-driven angiogenesis may be a more attractive therapeutic target and anti-HOHA-lactone therapy may be effective independently or as a complement to anti-VEGF or anti-CEP therapies for the inhibition of AMD. The present findings with HUVEC should only be extrapolated with caution. There are differences in the proliferative response of HUVEC and microvascular ECs to VEGF. The kinetics of the proliferative response to VEGF are different for micro and macrovascular cells.^{42, 43} On the other hand, it has been shown that VEGF receptors are inducible in vivo on venular and capillary ECs.⁴⁴ Thus, further studies are needed to define the precise responses of choroidal endothelial cells to the proangiogenic factors derived from docosahexanoate oxidation. Nevertheless, it is well known that VEGF plays a significant role in choroidal neovascularization, leading to the expectation based on our studies that the responses will be significant.

Supplementary Material

Refer to Web version on PubMed Central for supplementary material.

Acknowledgments

Funding Sources

This work was supported by NIH Grant R01-EY016813 to RGS.

ABBREVIATIONS

| | |
|----------------|--|
| AMD | age-related macular degeneration |
| ANOVA | analysis of variance |
| ARPE-19 | a human retinal pigmented epithelial cell line |
| CEP | 2-(ω -carboxyethyl)pyrrole |
| CM | conditioned medium |
| DCF | 2',7'-dichlorodihydrofluorescein |
| DCFHDA | 2',7'-dichlorofluorescein diacetate |
| DHA | docosahexaenoic acid |
| DMEM | Dulbecco's modified Eagle's medium |
| DPBS | Dulbecco's phosphate buffered saline |
| DMSO | dimethylsulfoxide |
| DTNB | 5,5'-dithio-bis(2-nitrobenzoic acid) |

| | |
|---------------------|--|
| ELISA | enzyme-linked immunosorbent assay |
| FBS | fetal bovine serum |
| GFR | growth factor-reduced |
| GSH | glutathione |
| HBSS | Hank's balanced salt solution |
| 4-HNE | 4-hydroxy-2-nonenal |
| HOHA | 4-hydroxy-7-oxo-hept-5-enoic acid |
| HOHA-lactone | 3-(5-oxotetrahydrofuran-2-yl)acrylaldehyde |
| hRPE | human primary retinal pigmented epithelial cells |
| HUVEC | human umbilical vein endothelial cells |
| LDH | lactate dehydrogenase |
| MDA | malondialdehyde |
| MTT | 3-(4,5-dimethylthiazol-2-yl)-2,5-diphenyltetrazolium bromide |
| OxPLs | oxidized phospholipids |
| PUFA | polyunsaturated fatty acid |
| ROS | reactive oxygen species |
| RPE | retinal pigmented epithelium |
| RtEBM | retinal pigmented epithelial cell basal medium |
| SPE | solid-phase extraction |
| TLR2 | Toll-like receptor 2 |
| VEGF | vascular endothelial growth factor |

References

1. Choudhary S, Xiao T, Srivastava S, Zhang W, Chan LL, Vergara LA, Van Kuijk FJ, Ansari NH. Toxicity and detoxification of lipid-derived aldehydes in cultured retinal pigmented epithelial cells. *Toxicol Appl Pharmacol.* 2005; 204:122–134. [PubMed: 15808518]
2. Zhang J, Zhao J, Bai Y, Huang L, Yu W, Li X. Effects of p75 neurotrophin receptor on regulating hypoxia-induced angiogenic factors in retinal pigment epithelial cells. *Mol Cell Biochem.* 2015; 398:123–134. [PubMed: 25200140]
3. SanGiovanni JP, Chew EY. The role of omega-3 long-chain polyunsaturated fatty acids in health and disease of the retina. *Prog Retin Eye Res.* 2005; 24:87–138. [PubMed: 15555528]
4. Watkins WM, McCollum GW, Savage SR, Capozzi ME, Penn JS, Morrison DG. Hypoxia-induced expression of VEGF splice variants and protein in four retinal cell types. *Exp Eye Res.* 2013; 116:240–246. [PubMed: 24076411]

5. Faby H, Hillenkamp J, Roeder J, Klettner A. Hyperthermia-induced upregulation of vascular endothelial growth factor in retinal pigment epithelial cells is regulated by mitogen-activated protein kinases. *Graefes Arch Clin Exp Ophthalmol*. 2014; 252:1737–1745. [PubMed: 25047875]
6. Karamysheva AF. Mechanisms of angiogenesis. *Biochemistry (Moscow)*. 2008; 73:751–762. [PubMed: 18707583]
7. Yancopoulos GD, Davis S, Gale NW, Rudge JS, Wiegand SJ, Holash J. Vascular-specific growth factors and blood vessel formation. *Nature*. 2000; 407:242–248. [PubMed: 11001067]
8. Witmer A. Vascular endothelial growth factors and angiogenesis in eye disease. *Prog Retin Eye Res*. 2003; 22:1–29. [PubMed: 12597922]
9. Ma W, Lee SE, Guo J, Qu W, Hudson BI, Schmidt AM, Barile GR. RAGE ligand upregulation of VEGF secretion in ARPE-19 cells. *Invest Ophthalmol Vis Sci*. 2007; 48:1355–1361. [PubMed: 17325184]
10. Folk JC, Stone EM. Ranibizumab therapy for neovascular age-related macular degeneration. *N Engl J Med*. 2010; 363:1648–1655. [PubMed: 20961248]
11. Caldwell RB, Bartoli M, Behzadian MA, El-Remessy AE, Al-Shabrawey M, Platt DH, Caldwell RW. Vascular endothelial growth factor and diabetic retinopathy: pathophysiological mechanisms and treatment perspectives. *Diabetes Metab Res Rev*. 2003; 19:442–455. [PubMed: 14648803]
12. Beatty S, Koh H-H, Phil M, Henson D, Boulton M. The Role of Oxidative Stress in the Pathogenesis of Age-Related Macular Degeneration. *Surv Ophthalmol*. 2000; 45:115–134. [PubMed: 11033038]
13. Choi J, Zhang W, Gu X, Chen X, Hong L, Laird JM, Salomon RG. Lysophosphatidylcholine is generated by spontaneous deacylation of oxidized phospholipids. *Chem Res Toxicol*. 2011; 24:111–118. [PubMed: 20973507]
14. Wang H, Linetsky M, Guo J, Choi J, Hong L, Chamberlain AS, Howell SJ, Howes AM, Salomon RG. 4-Hydroxy-7-oxo-5-heptenoic Acid (HOHA) Lactone is a Biologically Active Precursor for the Generation of 2-(omega-Carboxyethyl)pyrrole (CEP) Derivatives of Proteins and Ethanolamine Phospholipids. *Chem Res Toxicol*. 2015
15. Crabb JW, Miyagi M, Gu X, Shadrach K, West KA, Sakaguchi H, Kamei M, Hasan A, Yan L, Rayborn ME, Salomon RG, Hollyfield JG. Drusen proteome analysis: an approach to the etiology of age-related macular degeneration. *Proc Natl Acad Sci U S A*. 2002; 99:14682–14687. [PubMed: 12391305]
16. Gu X, Meer SG, Miyagi M, Rayborn ME, Hollyfield JG, Crabb JW, Salomon RG. Carboxyethylpyrrole protein adducts and autoantibodies, biomarkers for age-related macular degeneration. *J Biol Chem*. 2003; 278:42027–42035. [PubMed: 12923198]
17. Wang H, Guo J, West XZ, Bid HK, Lu L, Hong L, Jang GF, Zhang L, Crabb JW, Linetsky M, Salomon RG. Detection and biological activities of carboxyethylpyrrole ethanolamine phospholipids (CEP-EPs). *Chem Res Toxicol*. 2014; 27:2015–2022. [PubMed: 25380349]
18. West XZ, Malinin NL, Merkulova AA, Tischenko M, Kerr BA, Borden EC, Podrez EA, Salomon RG, Byzova TV. Oxidative stress induces angiogenesis by activating TLR2 with novel endogenous ligands. *Nature*. 2010; 467:972–976. [PubMed: 20927103]
19. Ebrahem Q, Renganathan K, Sears J, Vasanji A, Gu X, Lu L, Salomon RG, Crabb JW, Anand-Apte B. Carboxyethylpyrrole oxidative protein modifications stimulate neovascularization: Implications for age-related macular degeneration. *Proc Natl Acad Sci U S A*. 2006; 103:13480–13484. [PubMed: 16938854]
20. Wang H, Linetsky M, Guo J, Yu AO, Salomon RG. Metabolism of 4-hydroxy-7-oxo-5-heptenoic acid (HOHA) lactone by retinal pigmented epithelial cells. *Chem Res Toxicol* submitted. 2016
21. Kuroki M, Voest EE, Amano S, Beerepoot LV, Takashima S, Tolentino M, Kim RY, Rohan RM, Colby KA, Yeo KT, Adamis AP. Reactive oxygen intermediates increase vascular endothelial growth factor expression in vitro and in vivo. *J Clin Invest*. 1996; 98:1667–1675. [PubMed: 8833917]
22. Bir SC, Shen X, Kavanagh TJ, Kevil CG, Pattillo CB. Control of angiogenesis dictated by picomolar superoxide levels. *Free Radic Biol Med*. 2013; 63:135–142. [PubMed: 23685287]

23. Bergmann M, Holz F, Kopitz J. Lysosomal stress and lipid peroxidation products induce VEGF-121 and VEGF-165 expression in ARPE-19 cells. *Graefes Arch Clin Exp Ophthalmol*. 2011; 249:1477–1483. [PubMed: 21509530]
24. Cho M, Hunt TK, Hussain MZ. Hydrogen peroxide stimulates macrophage vascular endothelial growth factor release. *American Journal of Physiology - Heart and Circulatory Physiology*. 2001; 280:2357–2363.
25. Pollreisz A, Afonyushkin T, Oskolkova OV, Gruber F, Bochkov VN, Schmidt-Erfurth U. Retinal pigment epithelium cells produce VEGF in response to oxidized phospholipids through mechanisms involving ATF4 and protein kinase CK2. *Exp Eye Res*. 2013; 116:177–184. [PubMed: 24021586]
26. Ayalasmayajula SP, Kompella UB. Induction of vascular endothelial growth factor by 4-hydroxynonenal and its prevention by glutathione precursors in retinal pigment epithelial cells. *Eur J Pharmacol*. 2002; 449:213–220. [PubMed: 12167462]
27. Vatsyayan R, Chaudhary P, Sharma A, Sharma R, Rao Lelsani PC, Awasthi S, Awasthi YC. Role of 4-hydroxynonenal in epidermal growth factor receptor-mediated signaling in retinal pigment epithelial cells. *Exp Eye Res*. 2011; 92:147–154. [PubMed: 21134369]
28. Vatsyayan R, Lelsani PC, Chaudhary P, Kumar S, Awasthi S, Awasthi YC. The expression and function of vascular endothelial growth factor in retinal pigment epithelial (RPE) cells is regulated by 4-hydroxynonenal (HNE) and glutathione S-transferase A4-4. *Biochem Biophys Res Commun*. 2012; 417:346–351. [PubMed: 22155253]
29. Day RM, Suzuki YJ. Cell proliferation, reactive oxygen and cellular glutathione. *Dose Response*. 2005; 3:425–442.
30. Choi J, Laird JM, Salomon RG. An efficient synthesis of gamma-hydroxy-alpha,beta-unsaturated aldehydic esters of 2-lysophosphatidylcholine. *Bioorg Med Chem*. 2011; 19:580–587. [PubMed: 21123073]
31. Kalyanaraman B, Darley-Usmar V, Davies KJ, Dennery PA, Forman HJ, Grisham MB, Mann GE, Moore K, Roberts LJ 2nd, Ischiropoulos H. Measuring reactive oxygen and nitrogen species with fluorescent probes: challenges and limitations. *Free Radic Biol Med*. 2012; 52:1–6. [PubMed: 22027063]
32. Rahman I, Kode A, Biswas SK. Assay for quantitative determination of glutathione and glutathione disulfide levels using enzymatic recycling method. *Nat Protoc*. 2006; 1:3159–3165. [PubMed: 17406579]
33. Vandeputte C, Guizon I, Genestie-Denis I, Vannier B, Lorenzon G. A microtiter plate assay for total glutathione and glutathione disulfide contents in cultured/isolated cells: performance study of a new miniaturized protocol. *Cell Biol Toxicol*. 1994; 10:415–421. [PubMed: 7697505]
34. Liang CC, Park AY, Guan JL. In vitro scratch assay: a convenient and inexpensive method for analysis of cell migration in vitro. *Nat Protoc*. 2007; 2:329–333. [PubMed: 17406593]
35. Ponce ML. Tube formation: an in vitro matrigel angiogenesis assay. *Methods Mol Biol*. 2009; 467:183–188. [PubMed: 19301671]
36. Kalariya NM, Ramana KV, Srivastava SK, van Kuijk FJ. Carotenoid derived aldehydes-induced oxidative stress causes apoptotic cell death in human retinal pigment epithelial cells. *Exp Eye Res*. 2008; 86:70–80. [PubMed: 17977529]
37. Ayalasmayajula SP, Kompella UB. Induction of vascular endothelial growth factor by 4-hydroxynonenal and its prevention by glutathione precursors in retinal pigment epithelial cells. *Eur J Pharmacol*. 2002; 449:213–220. [PubMed: 12167462]
38. Enoiu M, Herber R, Wennig R, Marson C, Bodaud H, Leroy P, Mitrea N, Siest G, Wellman M. gamma-Glutamyltranspeptidase-dependent metabolism of 4-hydroxynonenal-glutathione conjugate. *Arch Biochem Biophys*. 2002; 397:18–27. [PubMed: 11747306]
39. Charvet C, Liao WL, Heo GY, Laird J, Salomon RG, Turko IV, Pikuleva IA. Isolevuglandins and mitochondrial enzymes in the retina: mass spectrometry detection of post-translational modification of sterol-metabolizing CYP27A1. *J Biol Chem*. 2011; 286:20413–20422. [PubMed: 21498512]

40. Charvet CD, Laird J, Xu Y, Salomon RG, Pikuleva IA. Posttranslational modification by an isolevuglandin diminishes activity of the mitochondrial cytochrome P450 27A1. *J Lipid Res.* 2013; 54:1421–1429. [PubMed: 23479405]
41. Charvet CD, Saadane A, Wang M, Salomon RG, Brunengraber H, Turko IV, Pikuleva IA. Pretreatment with pyridoxamine mitigates isolevuglandin-associated retinal effects in mice exposed to bright light. *J Biol Chem.* 2013; 288:29267–29280. [PubMed: 23970548]
42. Lang I, Hoffmann C, Olip H, Pabst MA, Hahn T, Dohr G, Desoye G. Differential mitogenic responses of human macrovascular and microvascular endothelial cells to cytokines underline their phenotypic heterogeneity. *Cell Prolif.* 2001; 34:143–155. [PubMed: 11380484]
43. Lang I, Pabst MA, Hiden U, Blaschitz A, Dohr G, Hahn T, Desoye G. Heterogeneity of microvascular endothelial cells isolated from human term placenta and macrovascular umbilical vein endothelial cells. *Eur J Cell Biol.* 2003; 82:163–173. [PubMed: 12751902]
44. Ferrara N, Houck K, Jakeman L, Leung DW. Molecular and biological properties of the vascular endothelial growth factor family of proteins. *Endocr Rev.* 1992; 13:18–32. [PubMed: 1372863]

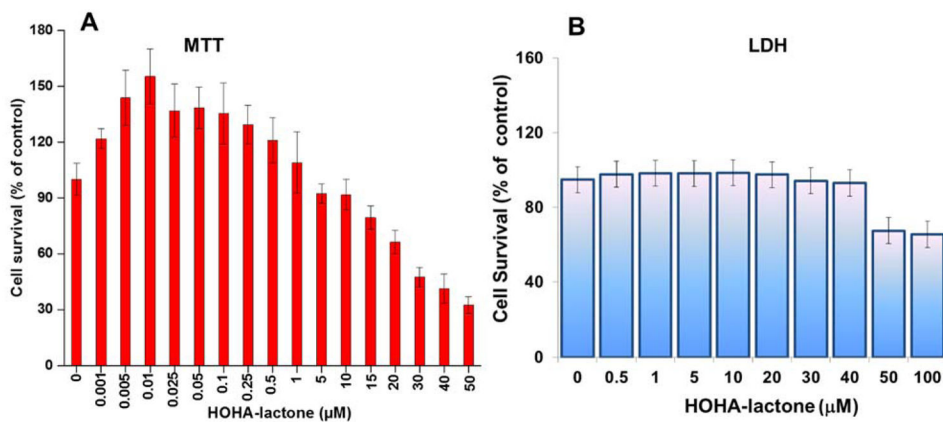


Figure 1. Effect of HOHA-lactone on survival of RPE cells. (A) ARPE-19 cells were treated with 0–100 μM of HOHA-lactone overnight (approximately 16 hours) and assayed for cytotoxicity by MTT (Panel A) and LDH assay (Panel B), respectively. Results are expressed as the percent cell survival (mean ± SD) relative to untreated ARPE-19 control cells (n = 8).

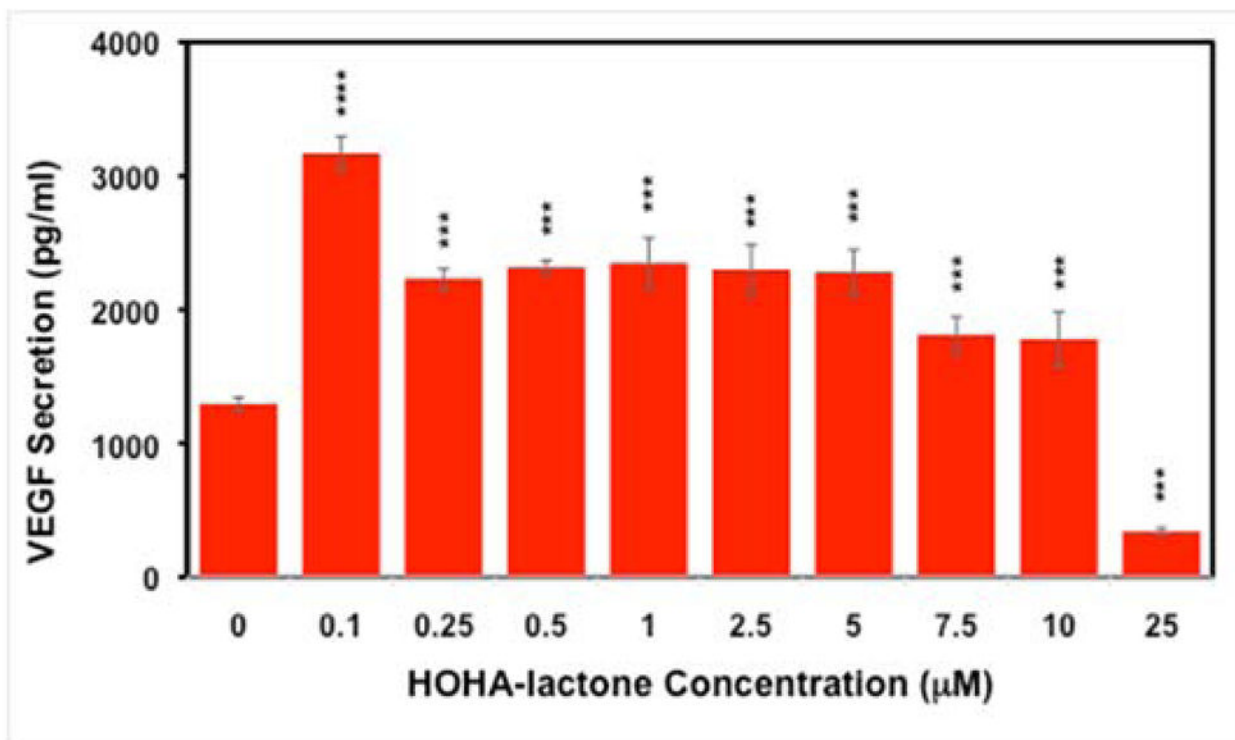


Figure 2. Effect of HOHA-lactone on VEGF secretion by ARPE-19 cells. Serum-starved ARPE-19 cells grown in a 96-well plate (25,000 cells per well) were treated with serum-free culture media containing varying concentrations (0–25 µM) of HOHA-lactone. After 16 h of incubation, supernatants were collected and secreted VEGF was measured using a human VEGF-A ELISA kit. The data represent the mean SD (n = 8) (“****” p<0.0001).

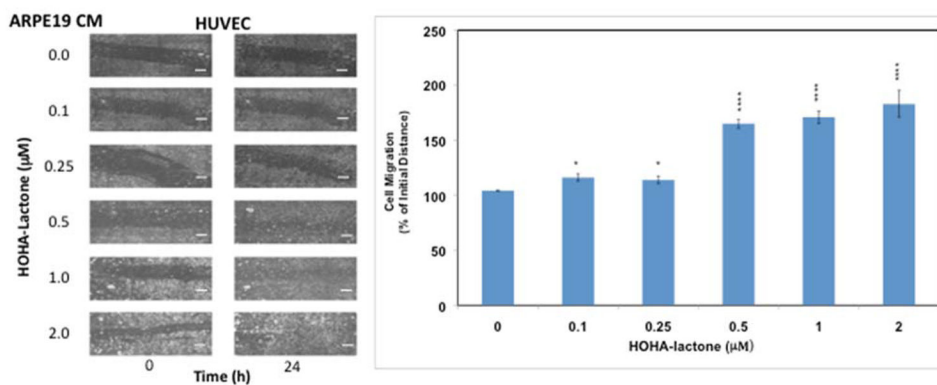


Figure 3. Effect of ARPE-19 cells conditioned medium on HUVEC in a wound healing assay. Left panel: representative phase-contrast images of cells with different treatment as indicated. Right panel: quantification of wound healing assay. The HUVEC monolayer (1×10^5 cells in $300 \mu\text{l}$ of a cell culture medium) was “injured” by a scratch with a sterile $200 \mu\text{L}$ pipette tip. The cells were incubated for 24 h in a CO_2 incubator in the presence of conditioned medium from control or HOHA-lactone-treated (0 – $2.0 \mu\text{M}$) ARPE-19 cells. Images are representative of four independent experiments showing very similar results. The data in bar graph represents the mean \pm SD ($n = 4$). Scale bars are $500.0 \mu\text{m}$.

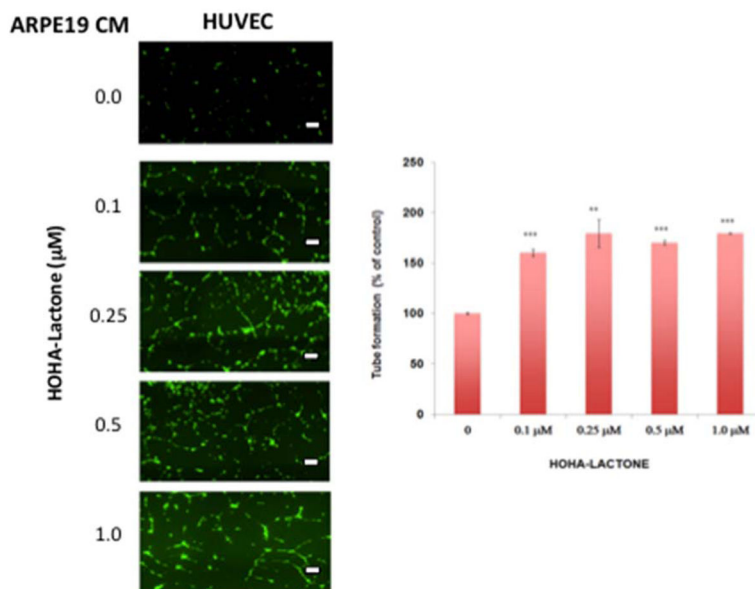


Figure 4. Effect of RPE conditioned medium on HUVEC in a tube formation assay. A: representative micrographs of cells with various treatments as indicated. B: quantification of tube formation assay. HUVEC (2.5×10^4 cells/well) in 24-flat bottom tissue culture plate were allowed to grow on RGF matrigel (175 μ L; approximately 15 mg/ml protein; 4 h) for 4 h in the presence of CM from ARPE-19 cells treated with 0–1 μ M of HOHA-lactone for another 16 h. The cells were stained with Calcein AM for 1 h at 37 $^{\circ}$ C in a CO₂ incubator. The images are representative of four experiments showing very similar results. The data in the bar graph represents the mean \pm SD (n = 4). Scale bars are 200.0 μ m.

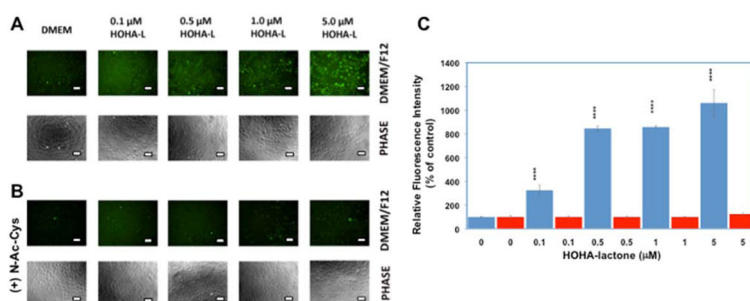


Figure 5. HOHA-lactone at submicromolar concentrations induces generation of intracellular reactive oxygen species in ARPE-19 cells. A: representative fluorescence (first row) and phase-contrast (second row) images of ARPE-19 cells treated with different HOHA-lactone concentrations for two hours under standard conditions as indicated. B: representative fluorescence (third row) and phase-contrast (fourth row) images of ARPE-19 cells pretreated with 10 mM N-Acetyl-Cys for 3 h, washed three times with warm DMEM/F12 basal medium and challenged with the same HOHA-lactone concentrations under conditions described in panel A. C: quantification of the fluorescence intensities. After DCFHDA pretreatment, ARPE-19 cells (4.5×10^4 cells) were further incubated with 0–1 μM HOHA-lactone before analysis. The images are representative of four independent experiments showing very similar results. The data in bar graph represents the mean \pm SD ($n = 4$). (“****” = $P < 0.00001$). Blue bars- no N-Ac-Cys was present in the cell culture medium; red bars- N-Ac-Cys was present in the cell culture medium. Scale bars are 25.0 μm.

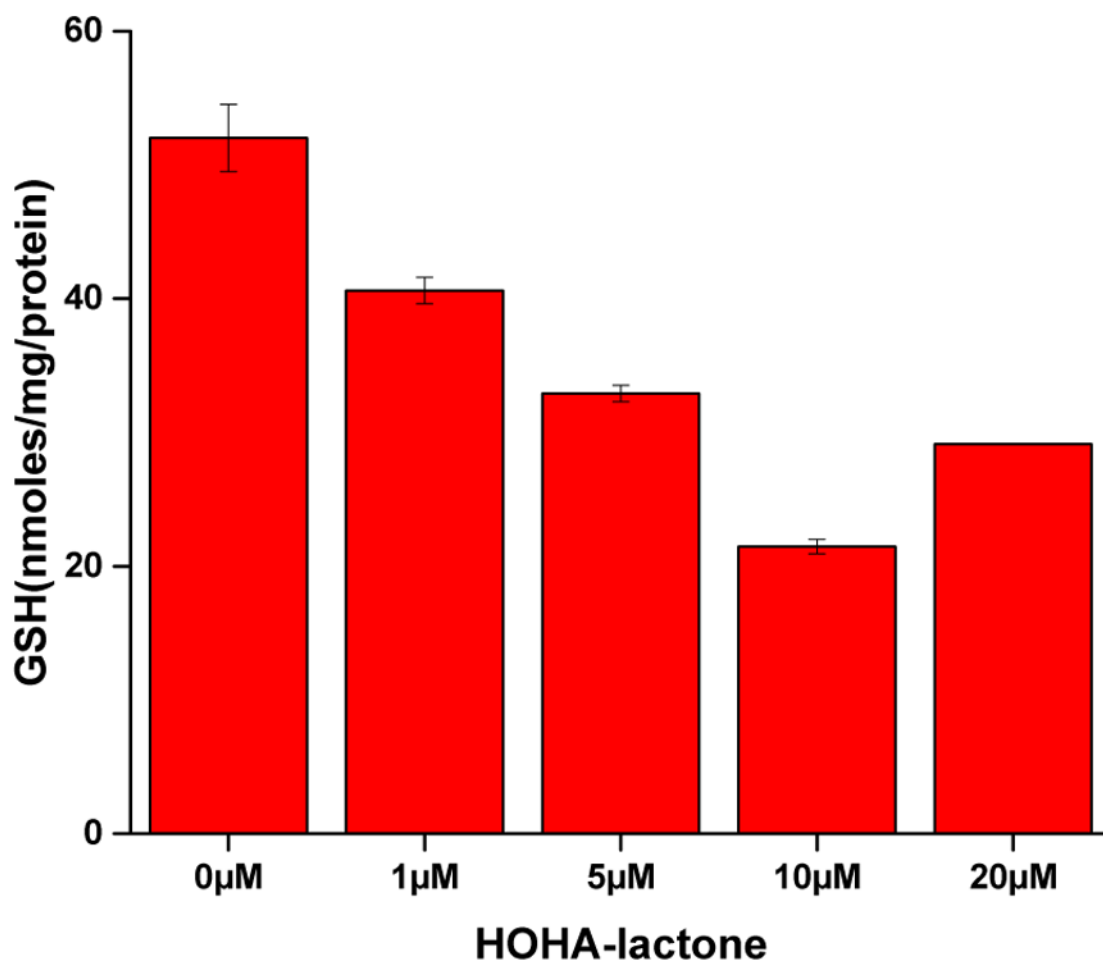


Figure 6. Dose-dependent effect of HOHA-lactone treatments on intracellular GSH levels in ARPE-19 cells. 2×10^6 cells were incubated with various concentrations of HOHA-lactone. After 2 h incubation, cells were harvested, lysed and sonicated. The level of intracellular GSH was determined by a colorimetric DTNB assay (see materials and methods above). Data are expressed as a mean \pm S.D for $n = 3$. Data shown are representative of three independent experiments that showed very similar results.

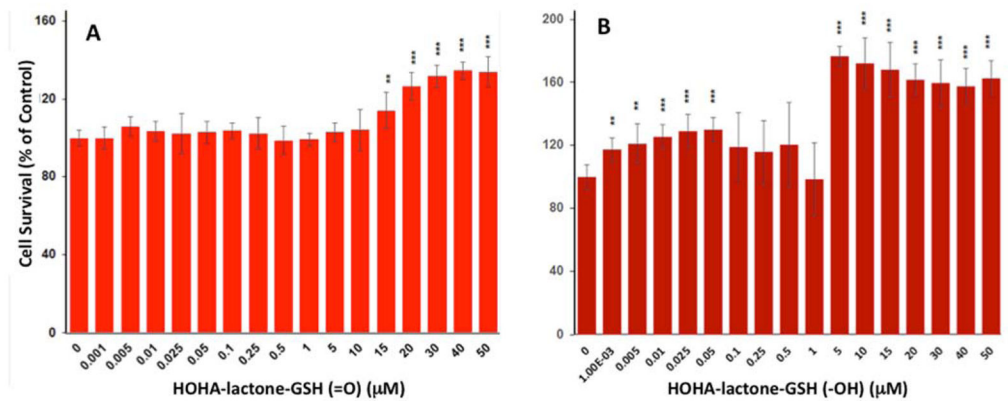


Figure 7. Concentration-dependent effect of HOHA-lactone-GSH (=O) (A) and HOHA-lactone-GSH (-OH) (B) on HUVEC cell viability. HUVEC were incubated with 0–50 μM HOHA-lactone-GSH conjugates overnight (approximately 16 hours) and then assayed for cytotoxicity by MTT. Results expressed as % of untreated control are means ± SD of independent experiments (n = 8).

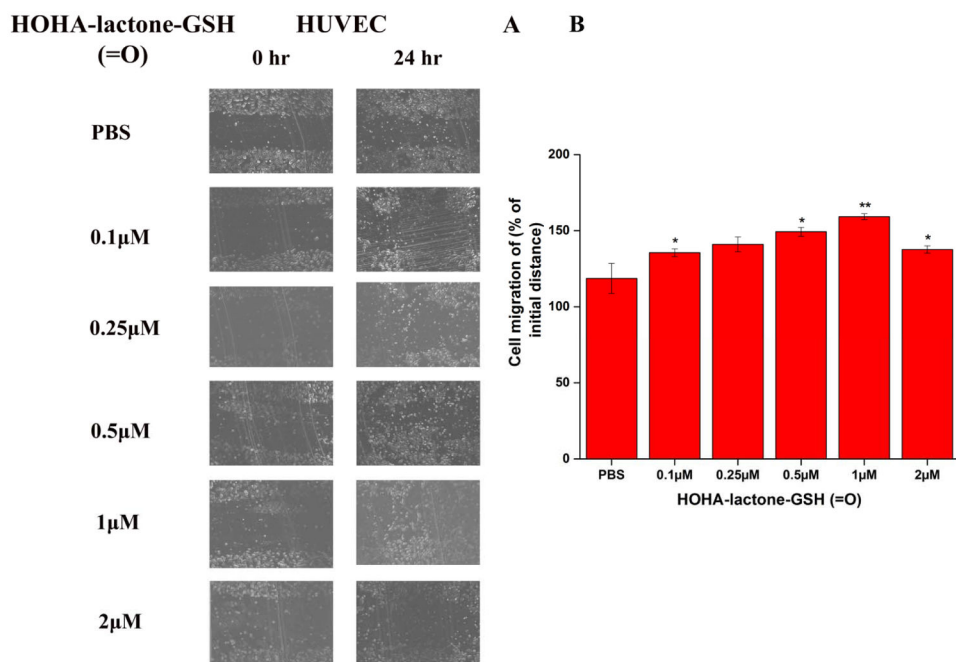


Figure 8.

The pro-angiogenic effect of HOHA-lactone-GSH (=O) on HUVEC in a wound healing assay. A: representative micrographs of cells with various treatments as indicated. B: quantification of the assay. HUVEC (1×10^5 cells in 300 μ l of a cell culture medium) were injured by a scratch with a 200 μ l pipette tip. Wounded cells were allowed to heal for 24 h in the presence of various concentrations of HOHA-lactone-GSH (=O) (0–2.0 μ M). The images are representative of four independent experiments showing very similar results. The data in bar graph represents the mean \pm SD (n = 4).

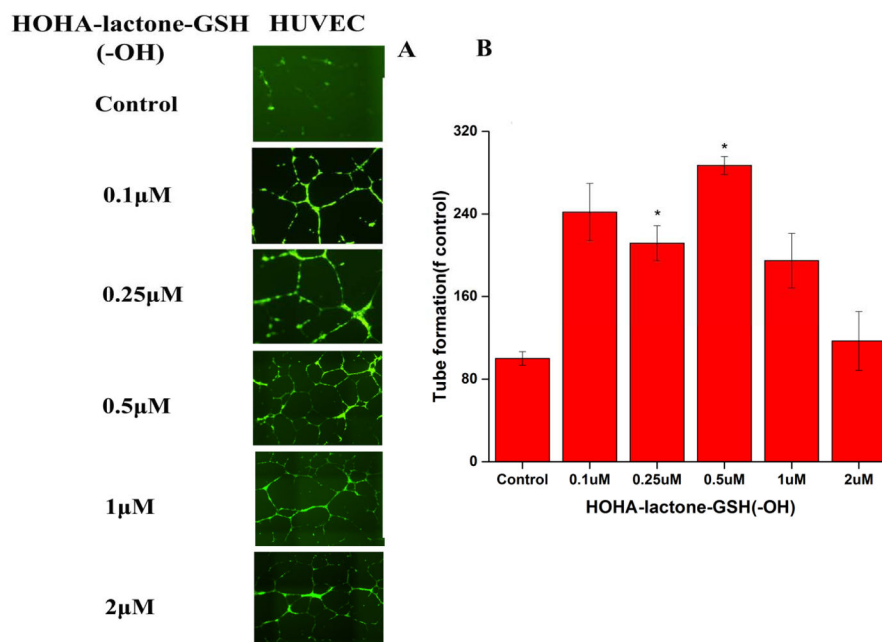


Figure 9. The pro-angiogenic effect of HOHA-lactone-GSH (-OH) on HUVEC in the tube formation assay. A: representative micrographs of cells with various treatments as indicated. B: quantification of the tube formation assay. HUVEC (2.5×10^4 cells/well) in 24-flat bottom tissue culture plate were allowed to grow on matrigel (175 μ L) for 4 h in presence of various concentrations of HOHA-lactone-GSH (-OH) (0–2.0 μ M) of HOHA-lactone for 16 h. The cells were then stained with Calcein AM for 1 h at 37 $^{\circ}$ C in a CO₂ incubator. The images are representative of four experiments showing very similar results. The data in the bar graph represents the mean \pm SD (n = 4).

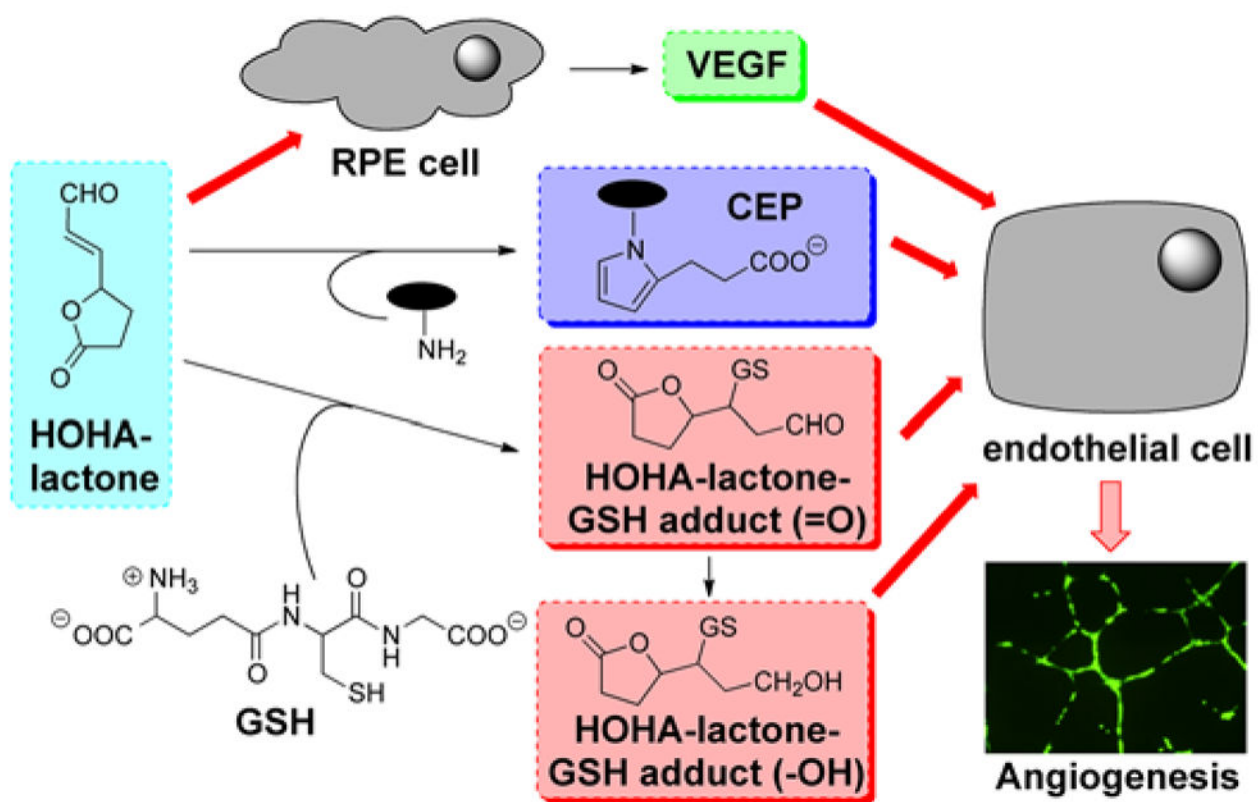
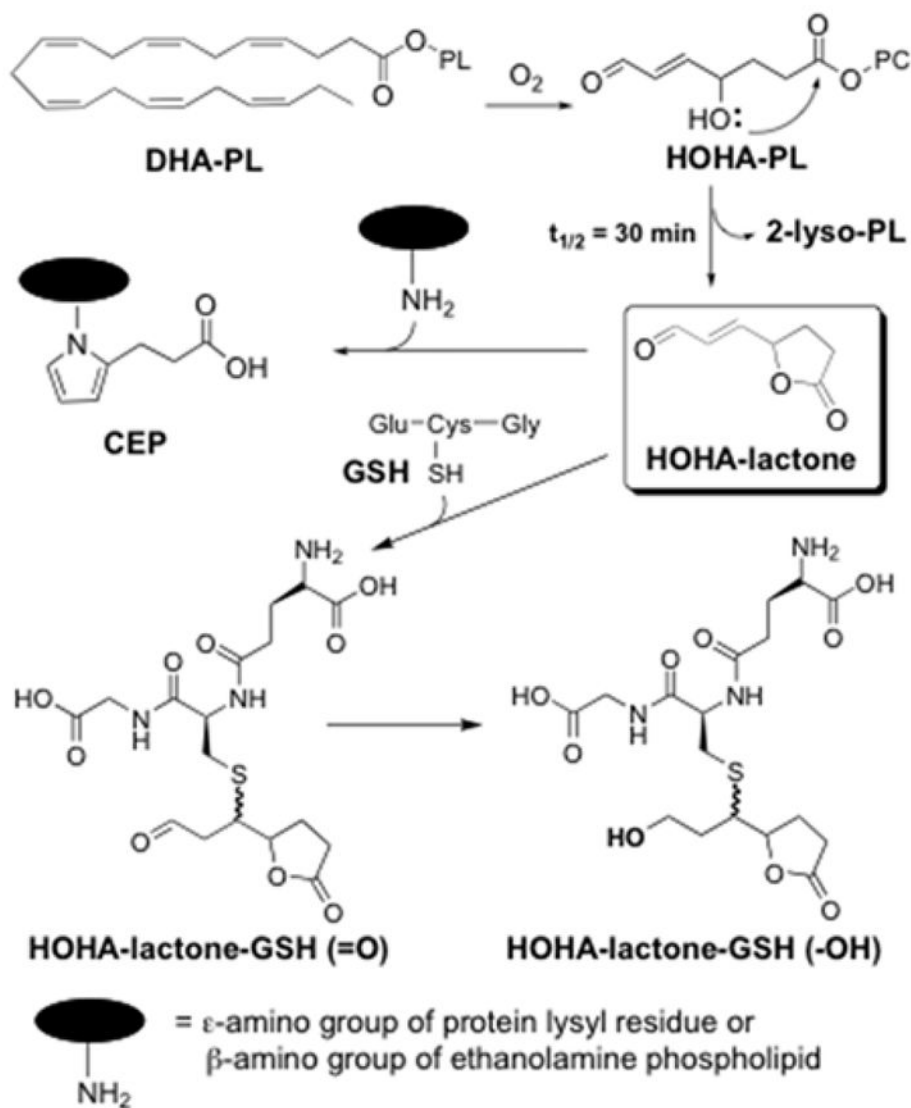


Figure 10.
Mechanisms for promotion of angiogenesis by HOHA-lactone.



Scheme 1.
Production of HOHA-lactone and its CEP- and GSH-derivatives.